

# Revealing Brown Carbon Chromophores Produced in Reactions of Methylglyoxal with Ammonium Sulfate

Peng Lin,<sup>†</sup> Julia Laskin,<sup>‡</sup> Sergey A. Nizkorodov,<sup>§</sup> and Alexander Laskin<sup>\*,†</sup>

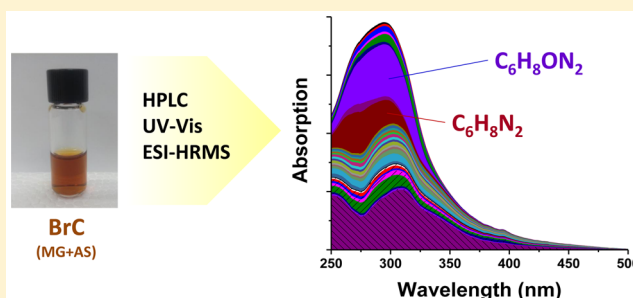
<sup>†</sup>Environmental Molecular Sciences Laboratory, Pacific Northwest National Laboratory, Richland, Washington 99354, United States

<sup>‡</sup>Physical Sciences Division, Pacific Northwest National Laboratory, Richland, Washington 99354, United States

<sup>§</sup>Department of Chemistry, University of California, Irvine, California 92697, United States

**S** Supporting Information

**ABSTRACT:** Atmospheric brown carbon (BrC) is an important contributor to light absorption and climate forcing by aerosols. Reactions between small water-soluble carbonyls and ammonia or amines have been identified as one of the potential pathways of BrC formation. However, detailed chemical characterization of BrC chromophores has been challenging and their formation mechanisms are still poorly understood. Understanding BrC formation is impeded by the lack of suitable methods which can unravel the variability and complexity of BrC mixtures. This study applies high performance liquid chromatography (HPLC) coupled to photodiode array (PDA) detector and high resolution mass spectrometry (HRMS) to investigate optical properties and chemical composition of individual BrC components produced through reactions of methylglyoxal (MG) and ammonium sulfate (AS), both of which are abundant in the atmospheric environment. A direct relationship between optical properties and chemical composition of 30 major BrC chromophores is established. Nearly all of these chromophores are nitrogen-containing compounds that account for >70% of the overall light absorption by the MG+AS system in the 300–500 nm range. These results suggest that reduced-nitrogen organic compounds formed in reactions between atmospheric carbonyls and ammonia/amines are important BrC chromophores. It is also demonstrated that improved separation of BrC chromophores by HPLC will significantly advance understanding of BrC chemistry.



## INTRODUCTION

Atmospheric brown carbon (BrC), which represents a poorly defined collection of particulate organic compounds that efficiently absorb solar radiation in the ultraviolet (UV) and visible (Vis) regions,<sup>1</sup> has a significant impact on the Earth's climate. BrC influences substantially or even dominates the total aerosol absorption at specific wavelengths in certain geographic areas.<sup>2–4</sup> It is known that light absorption by organic compounds strongly depends on their molecular structures.<sup>5</sup> However, understanding of the fundamental relationship between the chemical composition of BrC and its light absorption properties is still limited. Sources and emission factors of BrC are also complex and poorly characterized.<sup>6,7</sup> The lack of this knowledge does not allow accurate predictions by atmospheric models of BrC impact on climate.

BrC is generated from both primary emissions,<sup>1,8</sup> e.g., fossil fuel combustion<sup>9,10</sup> and biomass burning,<sup>11</sup> and a variety of secondary processes.<sup>7</sup> For instance, light-absorbing secondary organic aerosol (SOA) can be formed through photooxidation of aromatic volatile organic compounds (VOCs),<sup>12–14</sup> dehydration of oligomers formed through reactive uptake of isoprene epoxydiols,<sup>15</sup> and reactions of ammonia/amines with carbonyl compounds in SOA or cloud droplets.<sup>16–19</sup>

Furthermore, it has been proposed that part of light absorption properties of organic aerosols may be influenced by supra-molecular interactions resulting in formation of charge-transfer complexes,<sup>20</sup> the idea inspired by numerous experiments on chromophoric dissolved organic matter.<sup>21</sup>

One of the major analytical challenges in the characterization of BrC is employing a suitable separation procedure to distinguish the BrC chromophores from other aerosol constituents. It has been proposed that among the myriad constituents of particulate organic matter, BrC absorption may be controlled by a relatively small fraction of strongly absorbing molecules.<sup>22</sup> It has been also demonstrated that the optical properties of BrC may evolve significantly as a result of various atmospheric processes such as oxidation<sup>12,23</sup> and other chemical reactions,<sup>6</sup> solar irradiation,<sup>13,24</sup> changes in temperature<sup>25</sup> and relative humidity.<sup>18,26,27</sup> Therefore, obtaining molecular level information about individual BrC chromophores is critical to understanding their transformations by atmospheric aging processes and hence the underlying

Received: July 25, 2015

Revised: October 16, 2015

Accepted: October 27, 2015

Published: October 27, 2015

chemistry of BrC. Consequently, improved understanding of the BrC chemistry will be of practical use for constraining model estimates of BrC contribution to radiative forcing.<sup>28</sup>

The identification of individual light-absorbing constituents of organic aerosol is a challenging task that requires the combination of chromatographic separation techniques with sensitive and specific detectors.<sup>29</sup> The combination of high performance liquid chromatography (HPLC), photodiode array (PDA) detector, and high resolution mass spectrometry (HPLC/PDA/HRMS) is a powerful platform for chemical characterization of BrC aerosol. Previously, it has been successfully employed to identify and quantify several BrC chromophores in cloudwater<sup>30</sup> and atmospheric particulate samples.<sup>31–35</sup> In our previous work, nitro-aromatic chromophores in SOA generated through photooxidation of toluene in the presence of NO<sub>x</sub> were successfully separated using a reversed-phase C18 column.<sup>36</sup> However, in other cases,<sup>34,37</sup> the identified species contributed to a relatively small fraction of the overall light absorption by BrC, leaving a majority of the light-absorbing species unresolved. Furthermore, the commonly used C18 column did not adequately separate components of BrC containing reduced-nitrogen compounds generated by reaction of ketolimononaldehyde with ammonia.<sup>37</sup> Improved separation of these reduced-nitrogen species will advance our understanding of BrC chemistry. More broadly, it will improve understanding of other complex systems where color is the defining characteristic, such as natural pigments.

In this study, an extensively studied organic material produced by reactions of methylglyoxal (MG) with ammonium sulfate (AS) was selected as an atmospherically relevant complex BrC mixture.<sup>19,38–41</sup> Reactions between small water-soluble carbonyls and ammonia/amines such as MG and AS have been recognized as a potentially important pathway to BrC formation.<sup>16,18,19,37,42,43</sup> These reactions produce numerous reduced-nitrogen compounds making the identification of the individual chromophores challenging. This study is focused on the characterization of BrC chromophores in the MG+AS system. We optimize the experimental conditions for separation of BrC chromophores using six different HPLC columns and, using the best separation conditions, identify 30 abundant chromophores that account for more than 70% of the overall light absorption. In addition, our results provide practical recommendations for characterization of the BrC chromophores in atmospherically relevant mixtures containing reduced-nitrogen organic compounds.

## ■ EXPERIMENTAL SECTION

**Preparation of BrC Mixtures.** AS (>99.5%) and MG (40% wt. aqueous solution) were obtained from Acros Organics. Reactions of AS and MG were performed by following the procedures reported by Sareen et al.<sup>40</sup> It has been reported that the concentration of inorganic salt in atmospheric aerosols at typical relative humidity may exceed the bulk saturation point.<sup>44</sup> On the basis of this consideration and on the kinetics of BrC formation in MG+AS aqueous mixtures,<sup>41</sup> high concentration (~2M) aqueous AS solution was used for generating BrC material. Small volumes ( $\mu\text{L}$ ) of MG stock solution (40% wt. in water) were added to the AS solution to obtain the initial ~1 M concentration of MG in the mixed solution. This mole ratio of AS/MG was based on the upper bound concentration of MG<sup>45</sup> and the general concentration of AS in the atmosphere.<sup>46</sup> The aqueous mixture was stored under dark conditions and incubated at room temperature for ~96 h

prior to analysis. These browning reactions are known to take several days to reach completion; however, the dark brown color of the resulting solution after the incubation indicated formation of sufficient amount of BrC chromophores for the purposes of this study.

**HPLC/PDA/HRMS Instrumentation and Chromatographic Conditions.** BrC mixtures were analyzed using an HPLC/PDA/HRMS platform. The instrument consists of a Surveyor Plus system (including HPLC pump, autosampler and PDA detector), a standard IonMAX electrospray ionization (ESI) source, and a high resolution LTQ-Orbitrap mass spectrometer (all modules are from Thermo Electron, Inc.).

The six columns used for HPLC analysis were as follows: Phenomenex Luna C18(2), Phenomenex Synergi Fusion-RP, Phenomenex Synergi Hydro-RP, Phenomenex Kinetex Biphenyl, Thermo Scientific Synchronis HILIC, and Imtakt Scherzo SM-C18. Details about the specific vendor, column size, particle size, and other properties of these columns are summarized in Table S1 of the Supporting Information, SI. For HILIC column, the analysis was performed with isocratic elution using a 20:80 v/v mixture of H<sub>2</sub>O and CH<sub>3</sub>CN, at a flow rate of 200  $\mu\text{L min}^{-1}$ . The other five columns were operated at a flow rate of 200  $\mu\text{L min}^{-1}$  using the following elution protocol: a 3 min hold at 10% of CH<sub>3</sub>CN, a 43 min linear gradient to 90% CH<sub>3</sub>CN, a 7 min hold at this level, a 1 min return to 10% CH<sub>3</sub>CN, and another hold until the total scan time of 70 min. The SM-C18 column requires longer equilibration time; for this column the last step (10% CH<sub>3</sub>CN) was kept until 80 min. In most experiments, the column temperature was maintained at 25 °C and the sample injection volume was 2  $\mu\text{L}$ . Several experiments were carried out at column temperatures of 15 °C, as described below. UV–vis spectrum was measured using PDA detector over the wavelength range of 250 to 700 nm. The ESI settings were: positive ionization mode, + 4 kV spray potential, 35 units of sheath gas flow, 10 units of auxiliary gas flow, and 8 units of sweep gas flow.

**Data Analysis.** Xcalibur software (Thermo Scientific) was used to acquire raw data. Mass spectral features with a minimum signal-to-noise ratio of 10 were extracted using Decon2LS software<sup>47</sup> developed at Pacific Northwest National Laboratory (PNNL) (<http://ncrr.pnl.gov/software/>). Data processing was performed using a suite of Microsoft Excel macros that enable background subtraction and grouping of the mass spectral features using the first- and second-order mass defect analysis.<sup>48</sup> These procedures have been described in detail in our previous publications.<sup>48,49</sup> Elemental formulas were assigned to one peak in each group using MIDAS molecular formula calculator (<http://magnet.fsu.edu/~midas/>). Formula assignments were performed using the following constraints: C  $\leq$  50, H  $\leq$  100, N  $\leq$  5, O  $\leq$  50, S  $\leq$  2, and Na  $\leq$  1.

## ■ RESULTS AND DISCUSSION

The extent of chromatographic separation is crucial to the successful analysis of individual chromophores in BrC mixtures. HPLC separation can be affected by many factors, such as stationary phase and operation temperature of the column, pH, flow rate, and chemical composition of the mobile phase, etc.<sup>32,33,50–53</sup> Among them, selection of the best performing chromatographic column is most important to develop a robust HPLC methodology.<sup>50,51</sup> Thus, we conducted a systematic study to evaluate performance of six HPLC columns for separation of BrC chromophores in the MG+AS system. Figure

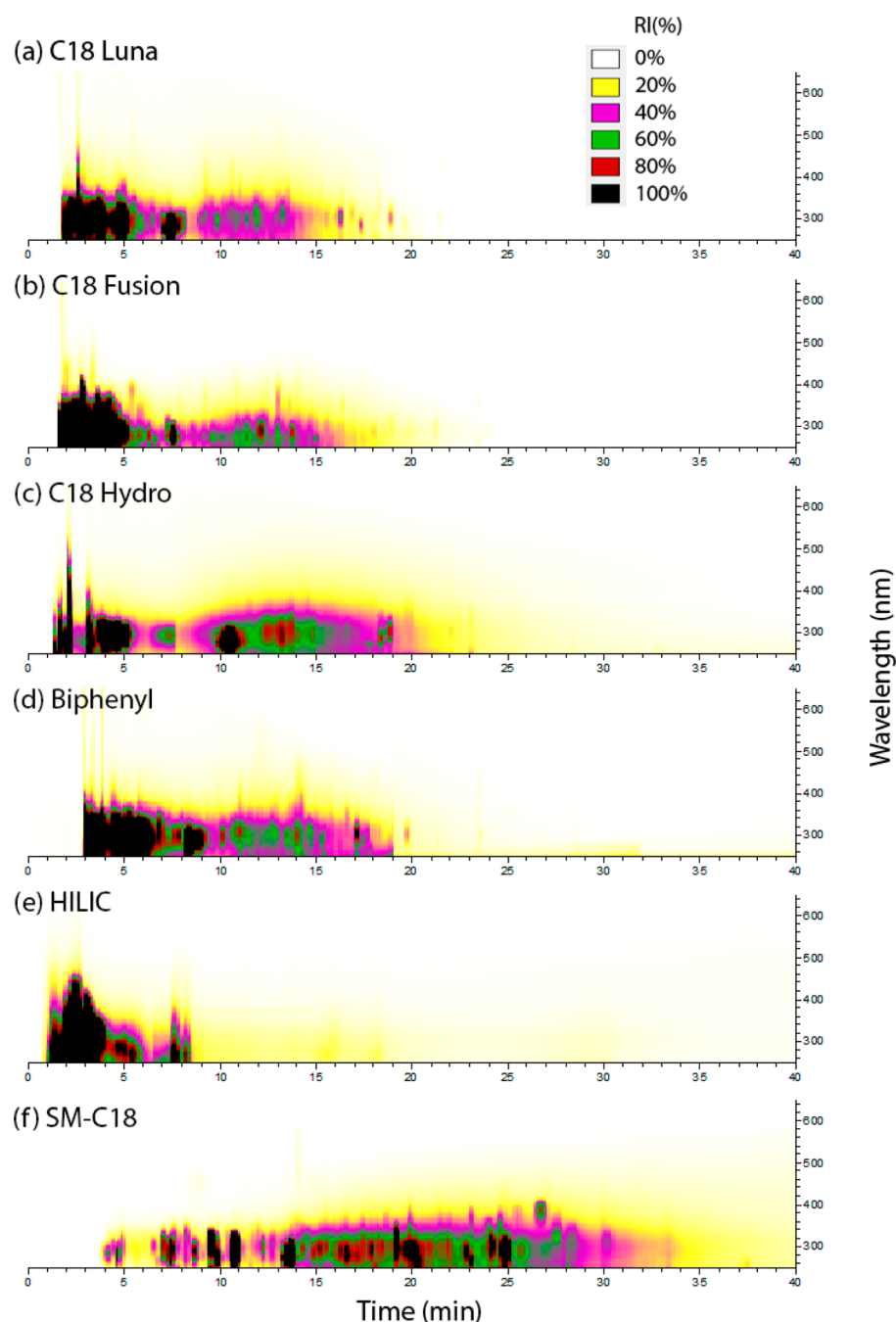


**Figure 1.** HPLC/PDA chromatograms of MG+AS mixture using six HPLC columns evaluated in this work. The x-axis is retention time, the y-axis is the UV-vis absorption wavelength and the color-coding denotes the relative intensity (RI) of light absorption.

1 displays the HPLC/PDA density maps of the BrC constituents eluted from six evaluated columns. It shows that the retention time of BrC chromophores varied among different columns. Detailed comparison of different columns is presented in Appendix I and Figure S1. In short, the best separation of the chromophores in this BrC mixture was achieved using the SM-C18 column. The commonly used reverse-phase (C18 Luna) column and the polar embedding modified (C18 Fusion) column showed inferior separation. The separation was partly improved with the use of polar end-capping (C18 Hydro) column and Biphenyl column. Separation on the HILIC column containing sulfoalkylbetaine zwitterions as the stationary phase was insufficient for the BrC mixture examined in this study.

The BrC material produced in reactions between MG and AS is a complex mixture. Its detailed chemical composition has not been fully described yet. However, it has been reported that the reactions between small  $\alpha$ -dicarbonyls and ammonia/amine tend to produce organic nitrogen compounds containing imidazole rings.<sup>16,18,19,37,38,40,42,43,54–56</sup> We examined extracted ion chromatograms (EICs) of several nitrogen-containing compounds in the MG+AS system. The elemental compositions of these compounds are listed and classified in Table S2. These compounds can be divided into three groups: (a) BrC compounds reported in other studies,<sup>40</sup> for which molecular structures were proposed based on the reported reaction mechanisms; (b) BrC compounds that have not been reported before, but for which their elemental formulas and structures

can be inferred based on previously reported reaction mechanisms and structurally related products;<sup>43,54–57</sup> and (c) light-absorbing nitrogen-containing compounds observed in this study for the first time. For the third group of compounds, only the elemental formulas are listed in the table; determination of their chemical structures is outside the scope of this paper. These compounds contain 6, 9, 12, or 15 carbon atoms and 1–3 nitrogen atoms. These products are dimers, trimers, tetramers, and pentamers of MG (which contains 3 carbon atoms) formed in its reactions with ammonia/ammonium.<sup>16,22</sup>

Figure 2 shows the EICs of the 17 compounds separated on the SM-C18 column. It should be pointed out that many

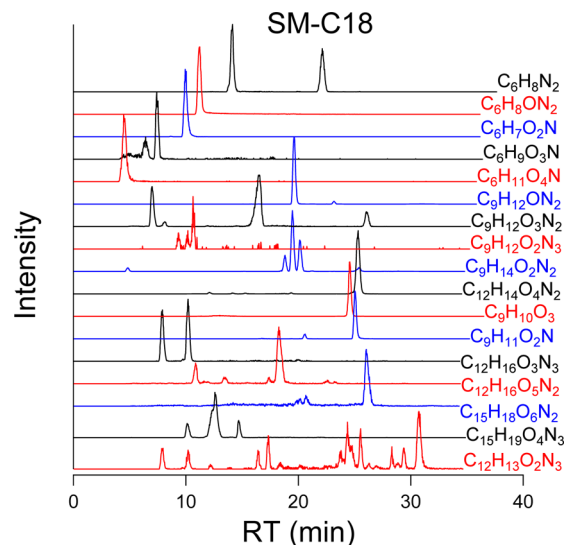


**Figure 2.** Extracted ion chromatograms (EICs) of 17 selected compounds in the MG+AS mixture separated by the SM-C18 column.

structural isomers may be associated with each assigned elemental formula. Indeed, some of the EICs contain several peaks eluting at different retention times (RTs); for example, the compound with formula  $C_{12}H_{13}O_2N_3$  has more than 10 peaks. Figure S2 shows the EICs of these compounds separated on other five columns. In agreement with the HPLC/PDA results shown in Figure 1, EICs indicate that best separation is obtained using the SM-C18 column. This is evident from the widest spread of the observed retention times for the tracked compounds.

The strength of interaction between the analyte and stationary phase of the HPLC column depends on the molecular structure, so some structural information about the observed BrC compounds can be inferred from their RTs on different HPLC columns. Specifically, some compounds (e.g.,  $C_6H_8ON_2$ ,  $C_9H_{12}ON_2$ ,  $C_{12}H_{14}O_4N_2$ ,  $C_9H_{10}O_3$ ,  $C_9H_{11}O_2N$ , and  $C_{12}H_{13}O_2N_3$ ) were efficiently separated using the conventional C18 Luna column (Figure S2a), indicating their nonpolar/hydrophobic properties. Less efficient separation was obtained using the C18 Fusion column, where most of the examined analytes coeluted within the first 5 min (Figure S2b). This is likely due to the presence of positive nitrogen-containing embedded groups on the surface of the stationary phase known to inhibit retention of basic analytes that experience ionic or dipole repulsion.<sup>58</sup> The C18 Hydro column retained more chromophores during 5–20 min of retention time compared with the other two C18 columns based on the

HPLC/PDA records (Figure S1). However, the EICs shown in Figure S2c suggest that the C18 Hydro column does not improve the retention of the examined nitrogen-containing compounds. This observation implies that the chromophores eluted during 5–20 min on the C18 Hydro column are different compounds compared to the ones listed in Table S2.

The low molecular weight  $C_6$  species ( $C_6H_8N_2$ ,  $C_6H_8ON_2$ ,  $C_6H_7O_2N$ ,  $C_6H_9O_3N$ , and  $C_6H_{11}O_4N$ ) were fully separated by the Biphenyl column (Figure S2d). Compounds with an imidazole ring (such as  $C_6H_8ON_2$ ) eluted later than the three compounds without rings in their structures ( $C_6H_7O_2N$ ,  $C_6H_9O_3N$ , and  $C_6H_{11}O_4N$ ), which is consistent with the propensity of the stationary phase of the Biphenyl column to retain aromatic compounds. The chemical structure of  $C_6H_8N_2$  is unknown, but its better retention by the Biphenyl column in comparison with  $C_6H_8ON_2$  indicates the presence of an aromatic ring in the structure. Similarly, on the basis of good retention of  $C_9H_{12}ON_2$ ,  $C_9H_{14}O_2N_2$ ,  $C_9H_{10}O_3$ , and  $C_9H_{11}O_2N$  species by this column, it is reasonable to assume that these compounds contain aromatic rings. Although compounds  $C_9H_{12}O_3N_2$  and  $C_9H_{13}O_2N_3$  were suggested to have an imidazole ring in their structures,<sup>40</sup> they eluted early from the Biphenyl column in comparison with other compounds. The reason for their poor retention on this column is not clear. One possible explanation is that they could be protonated in the eluent. This assumption is supported by the fact that the retention and separation of these two compounds were significantly improved on the SM-C18 column (Figure 2), which has ion exchange capability besides the reverse-phase interactions.

The results shown in Figures 2 and S2 also demonstrate that the MS signal of BrC chromophores strongly depends on the degree of HPLC separation. Because of different ionization efficiencies and competition of molecules for charge, quantification of individual compounds in complex mixtures using ESI-MS is challenging.<sup>59</sup> Efficient separation of compounds in complex mixtures prior to MS analysis reduces the effects of possible ion suppression during ionization. For example, it is shown that the signals of several oligomers (e.g.,  $C_{12}H_{16}O_3N_3$ ,  $C_{12}H_{16}O_5N_2$ ,  $C_{15}H_{18}N_2O_6$ , and  $C_{15}H_{19}O_4N_3$ ) are significantly suppressed in some cases due to their coelution with other compounds on the corresponding HPLC columns. In contrast, better separation of BrC compounds by the SM-C18 column resulted in improved chromatographic peak shape of these compounds presumably due to a decrease in ion suppression.

Although the SM-C18 column showed better capacity for resolving BrC chromophores, inorganic ions were also efficiently retained by this column because of its ion exchange capabilities (the inorganic ions eluted close to the dead time on other columns). Since the absorption bands of inorganic ions typical for ambient aerosols are usually below 250 nm wavelength,<sup>60</sup> the elution of inorganic ions does not affect the UV–vis spectrum of BrC chromophores. However, coelution of inorganic ions with organic compounds has a significant effect on the ionization efficiency of BrC chromophores and therefore on the intensity of the corresponding MS peaks. Figure S3 compares the HPLC-MS chromatograms and mass spectra of two BrC samples analyzed using the SM-C18 column. These two samples were prepared in the same bulk aqueous experiment and were divided into two equal parts. One part was subjected to a desalting procedure using the homogeneous liquid–liquid extraction method to extract

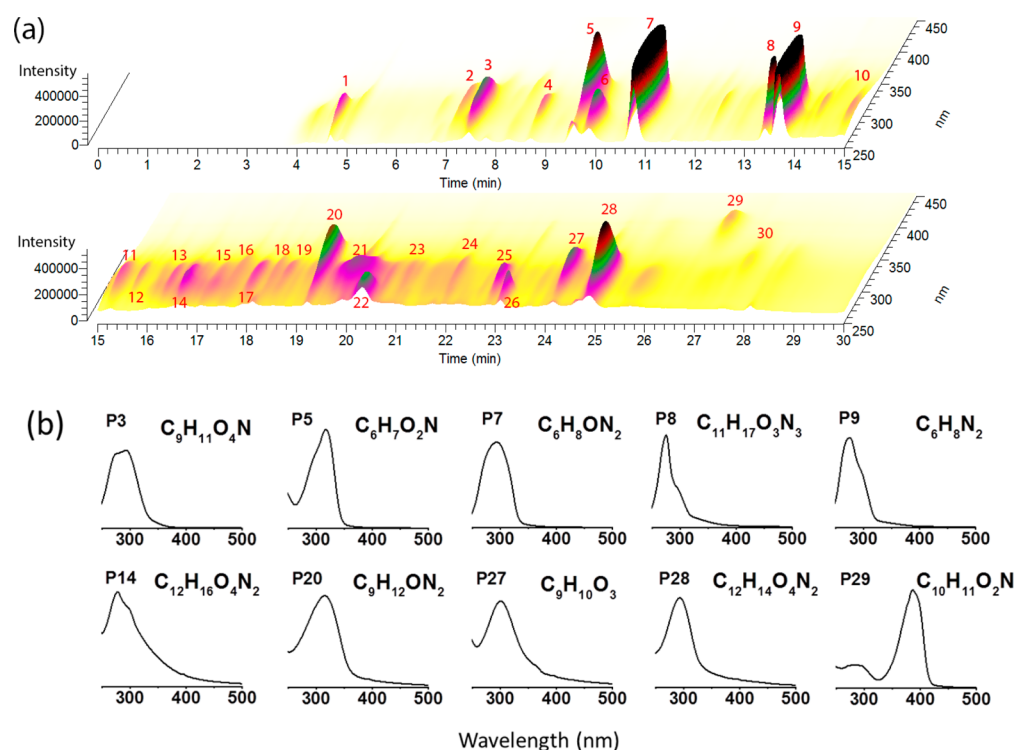


**Figure 3.** (a) HPLC/PDA chromatogram of the MG+AS mixture separated by the SM-C18 column. The numbers in red denote 30 BrC chromophores with well distinguished UV-vis spectra. (b) Selected examples of the UV-vis spectra from the above 30 chromophores (P#) and their corresponding elemental composition as inferred from HRMS.

organic compounds into  $\text{CH}_3\text{CN}$ .<sup>61</sup> Most of the AS was separated from the organic mixture due to its poor solubility in  $\text{CH}_3\text{CN}$ . The other part of the sample was diluted by pure water to achieve the same dilution ratio as in the desalted sample. It is shown that a larger number of peaks was observed in the chromatogram of the sample after desalting (Figure S3a). The mass spectra of the organic fractions eluted at different RT intervals were compared between these two samples (e.g., Figure S3b,c). In some cases, when no inorganic ions eluted, the mass spectra were almost identical between the two samples (e.g., Figure S3b). In other cases (e.g., Figure S3c,d), the mass spectra were significantly affected by the coelution of inorganic ions where MS signal of the target analytes was substantially suppressed. In that case, the presence of inorganic ions was unambiguously detected as a series of salt adducts with a constant mass difference. This result suggests that sample desalting prior to analysis is highly beneficial for sensitive detection of some target molecules.<sup>62</sup> However, desalting procedures should be used with care because they may remove some water-soluble aerosol components from the mixture, for example, isoprene-derived organosulfates and tetrols.<sup>63</sup>

Since the SM-C18 column showed best separation of BrC compounds in the MG+AS mixture, we examined the results obtained using this column in more detail. Figure 3a shows a 3D-plot of the signal from PDA detector as a function of retention time and light wavelength. It is shown that at least 30 PDA peaks (i.e., BrC chromophores) were well resolved. Good separation allowed us to extract UV-vis spectra of the individual chromophores from the HPLC/PDA data. After correcting for the shift in retention times between the signals recorded by MS and PDA detectors, mass spectra corresponding to the 30 peaks denoted in Figure 3a were investigated using similar procedures reported in our previous study.<sup>36</sup>

Elemental formulas of these compounds were determined based on the accurate mass measurement. In a number of cases, only one major ion was observed in the mass spectrum associated with a specific PDA peak. Examples of these compounds and their corresponding UV-vis spectra are shown in Figure 3b. A majority of chromophores in the MG+AS system exhibit their maximum light absorption wavelength around 300 nm. One exception is  $\text{C}_{10}\text{H}_{11}\text{O}_2\text{N}$  (peak #29), which has an absorption maximum at  $\sim 380$  nm.

Figure 4 shows the relative contribution to the UV-vis absorption by the 30 BrC chromophores denoted in Figure 3a with respect to the total light absorption by the MG+AS mixture. On average, light absorption by these 30 chromophores accounts for  $>70\%$  of the overall absorbance in the 300–500 nm range. Of note, some BrC compounds may interact with the stationary-phase of the column trapping them permanently. In order to account for such losses, total light absorption of this BrC mixture was measured by the photodiode array (PDA) detector of the HPLC system without column separation. Table 1 lists the elemental formulas of compounds with EICs associated with these BrC chromophores. Most of them are nitrogen-containing compounds, which highlights the significant contribution of reduced-nitrogen species to the overall BrC absorption by the MG+AS mixture. Formation of light-absorbing compounds in the mixtures of  $\alpha$ -dicarbonyls and ammonia/amines has been proposed in previous studies.<sup>26,40,64–67</sup> Specifically, oligomerization of  $\alpha$ -dicarbonyls catalyzed by inorganic salts and C–N bond formation were suggested as the pathways of BrC formation.<sup>67</sup> The former mainly generates CHO oligomers (containing only carbon, hydrogen and oxygen atoms) through aldol condensation and/or hemiacetal formation; whereas the latter forms reduced N-containing compounds such as amines,

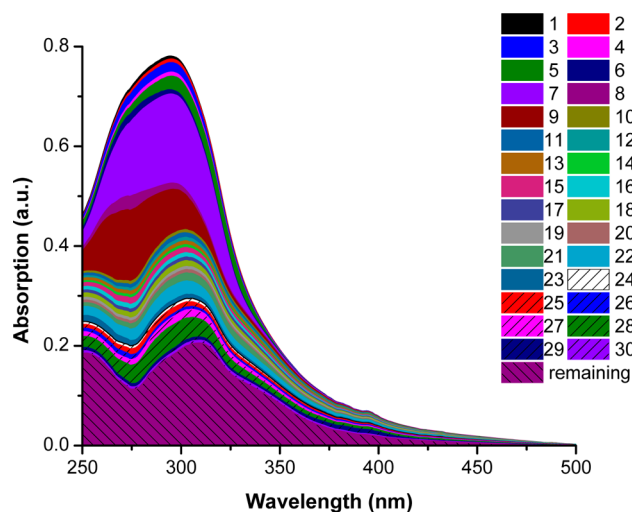


**Figure 4.** Relative contribution of 30 PDA peaks in the MG+AS mixture denoted in Figure 3 with respect to the total light absorption by the MG+AS mixture recorded in the PDA measurement without column separation.

primary and secondary (Schiff bases) imines and imidazoles. Formulas listed in Table 1 contain up to 3 nitrogen atoms, 0–7 oxygen atoms and 6–18 carbon atoms, suggesting the contributions from both pathways.

The number of carbon atoms in some of the compounds deviate from the  $n \times C3$  pattern expected for oligomerization reactions of the MG reactant. It follows that more complicated mechanisms, possibly involving autoxidation products by dissolved oxygen, operate in the slowly brewing MG+AS mixture. For example, the  $C_{10}H_{11}O_2N$  chromophore (peak #29) with an absorption maximum at  $\sim 380$  nm has ten carbon atoms requiring three MG units and an additional carbon atom for its assembly. This is similar to the reaction of ketolimononaldehyde ( $C_9H_{14}O_3$ ) with ammonia, which produced a number of products deviating from the expected  $n \times C9$  sequence.<sup>37</sup>

Formation of light-absorbing CHO oligomers has been previously observed in reactions of  $\alpha$ -dicarbonyls and ammonium salts.<sup>40,66</sup> However, among the 30 major chromophores observed in this study, only chromophore #27 corresponding to the CHO oligomer ( $C_9H_{10}O_3$ ) exhibits significant absorbance. In addition,  $C_{10}H_{14}O_4$  compound was observed as peak #10, but we cannot unambiguously identify it as a chromophore since it coeluted with  $C_{15}H_{19}O_6N$  species. Overall, our results indicate that CHO oligomers are not the major BrC chromophores in the MG+AS system.

The most abundant peaks in Figure 3a (#7, #9, #5, and #28) correspond to  $C_6H_8ON_2$ ,  $C_6H_8N_2$ ,  $C_6H_7O_2N$ , and  $C_{12}H_{14}O_4N_2$ . The contributions of these four chromophores to the total light absorption are much more pronounced in the UV region, while their contribution to light absorption in the visible range is similar to other smaller peaks (Figure 4). This result suggests that, in the MG+AS system, the light absorption in the visible range (i.e., above 400 nm) is contributed by many weakly absorbing chromophores. This observation is consistent with previous UV–vis studies of bulk mixtures formed in reactions of  $\alpha$ -dicarbonyls with ammonia. In such systems, light absorption is centered in the UV range (below 400 nm)<sup>19,66</sup> and absorbance in the visible range originates from an extended tail of the major UV peaks.<sup>40</sup> In contrast, another type of BrC

**Table 1.** Elemental Formulas of Compounds with EICs Associated with 30 PDA Peaks Denoted in Figures 3 and 4

peak #	$\lambda_{max}$ (nm)	measured $m/z$	neutral formula <sup>c</sup>	DBE <sup>b</sup>
1	283	235.10712	$C_{12}H_{14}O_3N_2$	7
2	304	144.06535	$C_6H_9O_3N$	3
3	294	198.07560	$C_9H_{11}O_4N$	5
4	290	223.10704	$C_{11}H_{14}O_3N_2$	6
5	317	126.05478	$C_6H_7O_2N$	4
6	273	<b>250.11920</b>	$C_{12}H_{15}O_3N_3$	7
		280.07834	$C_{11}H_{15}O_6N^a$	5
7	290	125.07069	$C_6H_8ON_2$	4
8	275	240.13362	$C_{11}H_{17}O_3N_3$	5
9	267	109.07584	$C_6H_8N_2$	4
10	285	199.09596	$C_{10}H_{14}O_4$	4
		<b>310.12772</b>	$C_{15}H_{19}O_6N$	7
11	296	192.11270	$C_{10}H_{13}ON_3$	6
		<b>264.13373</b>	$C_{13}H_{17}O_3N_3$	7
		362.17007	$C_{18}H_{23}O_3N_3$	9
12	299	<b>299.12289</b>	$C_{13}H_{18}O_6N_2$	6
		340.14932	$C_{15}H_{21}O_6N_3$	7
13	289	182.08073	$C_9H_{11}O_3N$	5
14	278	253.11765	$C_{12}H_{16}O_4N_2$	6
15	278	276.13333	$C_{14}H_{17}O_3N_3$	8
		<b>328.13818</b>	$C_{15}H_{21}O_7N$	6
16	299	138.09117	$C_8H_{11}ON$	4
17	294	<b>233.12781</b>	$C_{13}H_{16}O_2N_2$	7
		269.11243	$C_{12}H_{16}O_3N_2$	6
18	301	162.10225	$C_9H_{11}N_3$	6
		178.09712	$C_9H_{11}ON_3$	6
		<b>227.10196</b>	$C_{10}H_{14}O_4N_2$	5
19	301	139.08646	$C_7H_{10}ON_2$	4
20	315	165.10191	$C_9H_{12}ON_2$	5
21	294	288.13351	$C_{15}H_{17}O_3N_3$	9
		349.13858	$C_{17}H_{20}O_6N_2$	9
22	261	239.10204	$C_{11}H_{14}O_4N_2$	6
23	299	150.05472	$C_8H_7O_2N$	6
24	303	318.13257	$C_{17}H_{19}O_3N$	9
25	286	<b>151.08626</b>	$C_8H_{10}ON_2$	5
		365.13354	$C_{17}H_{20}O_7N_2$	9
26	272, 366	245.12766	$C_{14}H_{16}O_2N_2$	8
27	300	167.06998	$C_9H_{10}O_3$	5
28	293	251.10199	$C_{12}H_{14}O_4N_2$	7
29	386	178.08593	$C_{10}H_{11}O_2N$	6
30	322	<b>153.10199</b>	$C_8H_{12}ON_2$	4
		170.08087	$C_8H_{11}O_3N$	4
		180.06514	$C_9H_9O_3N$	6

<sup>a</sup>denote the molecules detected in the form of  $[M + Na]^+$  ions. <sup>b</sup>The double-bond equivalent (DBE) values for the neutral formulas were calculated using the equation:  $DBE = c - h/2 + n/2 + 1$ , where  $c$ ,  $h$ , and  $n$  correspond to the number of carbon, hydrogen and nitrogen atoms in the neutral formula, respectively; assuming that the positive mode mass spectral features were either protonated  $[M + H]^+$  or sodiated  $[M + Na]^+$  molecules. <sup>c</sup>Formulas marked by bold characters denote the abundant ion when multiple ions were associated with the same BrC chromophore.

mixture produced from limonene SOA reacting with ammonia exhibits a distinct peak in the absorption spectrum in the visible range ( $\sim 500$  nm),<sup>16,37</sup> and its light absorption properties are consistent with the minor presence of strongly absorbing chromophores.<sup>22</sup> This difference implies the existence of other efficient browning reaction mechanisms in addition to those involving  $\alpha$ -dicarbonyls.

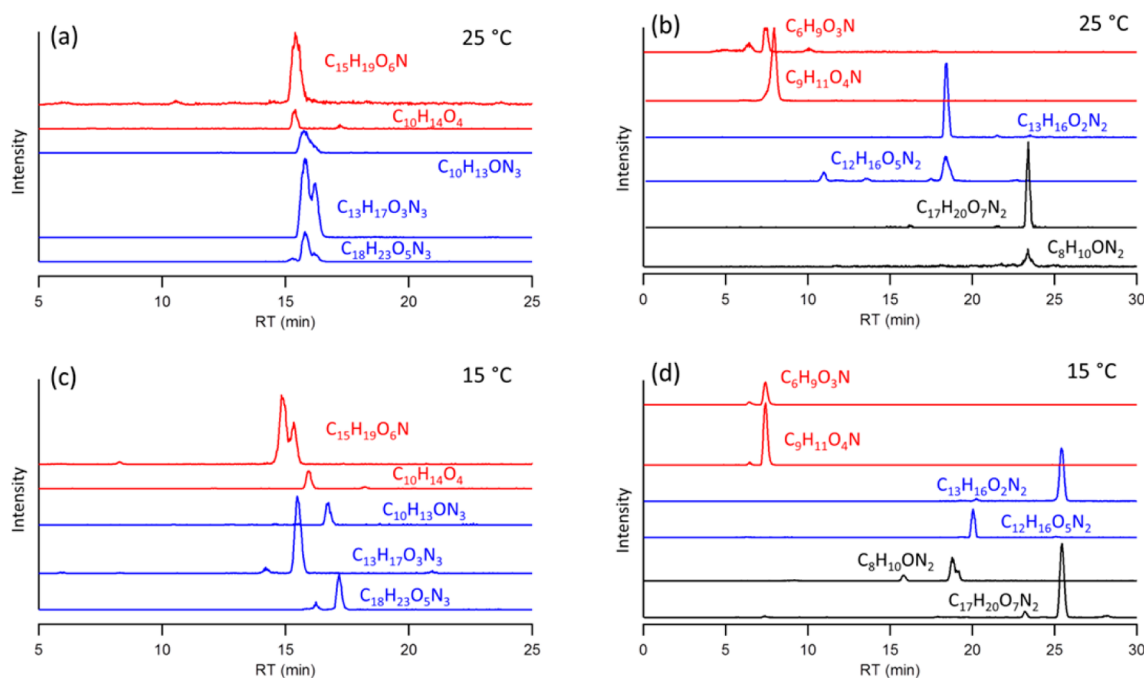


**Figure 5.** EICs of selected ions obtained by HPLC/HRMS analysis operated at different column temperatures: (a) and (b), 25 °C; and (c) and (d), 15 °C. EICs of ions in panel (a) correspond to peak 10 (red) and peak 11 (blue) listed in Table 1. EICs of ions in panel (b) correspond to peak 2 and 3 (red), peak 17 (blue), and peak 25 (black). Panels (c) and (d) show the EICs of these ions obtained by HPLC analysis when the column temperature was set at 15 °C.

Table 1 indicates that in some cases multiple molecules are associated with a single PDA peak (e.g., peaks #10, 11, 17, 25). This could be caused by in-source fragmentation of the chromophore or coelution of insufficiently separated compounds. In order to distinguish between these two scenarios, additional experiments were conducted at the column temperature of 15 °C as shown in Figure 5. The coeluted peaks at 25 °C were separated from each other at 15 °C, indicating that insufficient separation is mainly responsible for the presence of multiple molecules in the same PDA peak. However, additional coeluted peaks were also observed at 15 °C. For example,  $C_6H_9O_3N$  and  $C_9H_{11}O_4N$  were well separated at 25 °C (Figure 5b), but coeluted at 15 °C (Figure 5d). This confirms the well-known fact that complete separation of complex organic mixtures such as organic aerosol with one-dimensional HPLC is challenging. The extent of separation can be improved by acquiring chromatograms at different temperatures or on different columns. Further separation may also be achieved with two-dimensional (2D) HPLC through the combination of two columns with different stationary phases. Of note, 2D-HPLC requires much longer analysis time and also increases the data processing workload.<sup>68</sup>

The results presented here demonstrate that light absorption by BrC in the MG+AS mixture can be adequately accounted for by ~30 major chromophores. Combined with previous reports,<sup>16,18,19,37,38,40,42,43,54–56</sup> our study indicates that major BrC chromophores in the MG+AS mixture correspond to reduced-nitrogen compounds formed in reactions between  $\alpha$ -dicarbonyls and ammonia/amines. Additional field and laboratory studies are required to better understand the properties and formation mechanisms of the reduced-nitrogen species and quantify their effect on the light absorption by atmospheric BrC. Furthermore, it is important to estimate the concentrations of such BrC chromophores in atmospheric organic aerosols. This may be achieved using either

commercially available standards or surrogate compounds representing a particular class of reduced-nitrogen species (e.g., imidazoles, primary amines, etc.). Furthermore, it will be important in the future to expand the application of the method to the analysis of other BrC mixtures formed in reactions of organic aerosols with ammonia/amines.

## ■ ASSOCIATED CONTENT

### 📄 Supporting Information

The Supporting Information is available free of charge on the ACS Publications website at DOI: 10.1021/acs.est.5b03608.

Additional description of experimental procedures and results: Table S1 lists specifications of the six evaluated HPLC columns and Appendix I describes analytical chemistry aspects of separation by these columns; Table S2 lists organic compounds detected in the MG+AS mixture; Figure S1 shows fractions of the overall HPLC/PDA signals detected at different elution periods by different columns; Figure S2 compares EICs of the 17 selected products MG+AS mixtures separated by different columns; Figure S3 illustrates the effect of sample desalting on the performance of the SM-C18 column for separating constituents of MG+AS mixtures (PDF)

## ■ AUTHOR INFORMATION

### Corresponding Author

\*Phone: +1 (509) 3716129; e-mail: alexander.laskin@pnnl.gov (A.L.).

### Notes

The authors declare no competing financial interest.

## ■ ACKNOWLEDGMENTS

We acknowledge support by the U.S. Department of Commerce, National Oceanic and Atmospheric Administration

through Climate Program Office's AC4 program, awards NA13OAR4310066 and NA13OAR4310062. The HPLC/PDA/ESI-HRMS measurements were performed at the W.R. Wiley Environmental Molecular Sciences Laboratory (EMSL), a national scientific user facility located at PNNL, and sponsored by the Office of Biological and Environmental Research of the U.S. DOE. PNNL is operated for US DOE by Battelle Memorial Institute under Contract No. DEAC06-76RL0 1830.

## REFERENCES

- (1) Andreae, M. O.; Gelencser, A. Black carbon or brown carbon? The nature of light-absorbing carbonaceous aerosols. *Atmos. Chem. Phys.* **2006**, *6*, 3131–3148.
- (2) Bahadur, R.; Praveen, P. S.; Xu, Y. Y.; Ramanathan, V. Solar absorption by elemental and brown carbon determined from spectral observations. *Proc. Natl. Acad. Sci. U. S. A.* **2012**, *109* (43), 17366–17371.
- (3) Chung, C. E.; Ramanathan, V.; Decremer, D. Observationally constrained estimates of carbonaceous aerosol radiative forcing. *Proc. Natl. Acad. Sci. U. S. A.* **2012**, *109* (29), 11624–11629.
- (4) Ramanathan, V.; Li, F.; Ramana, M. V.; Praveen, P. S.; Kim, D.; Corrigan, C. E.; Nguyen, H.; Stone, E. A.; Schauer, J. J.; Carmichael, G. R.; Adhikary, B.; Yoon, S. C. Atmospheric brown clouds: Hemispherical and regional variations in long-range transport, absorption, and radiative forcing. *J. Geophys. Res.*, 2007, *112*, (D22), D22S21, DOI: [10.1029/2006JD008124](https://doi.org/10.1029/2006JD008124).
- (5) Turro, N. J.; Ramamurthy, V.; Scaiano, J. C. *Modern Molecular Photochemistry of Organic Molecules*; University Science Books: Sausalito, CA, 2010, 1110 pages.
- (6) Laskin, A.; Laskin, J.; Nizkorodov, S. A. Chemistry of Atmospheric Brown Carbon. *Chem. Rev.* **2015**, *115* (10), 4335–4382.
- (7) Moise, T.; Flores, J. M.; Rudich, Y. Optical properties of secondary organic aerosols and their changes by chemical processes. *Chem. Rev.* **2015**, *115* (10), 4400–4439.
- (8) Bond, T. C.; Bergstrom, R. W. Light absorption by carbonaceous particles: An investigative review. *Aerosol Sci. Technol.* **2006**, *40* (1), 27–67.
- (9) Bond, T. C. Spectral dependence of visible light absorption by carbonaceous particles emitted from coal combustion. *Geophys. Res. Lett.* **2001**, *28* (21), 4075–4078.
- (10) Hecobian, A.; Zhang, X.; Zheng, M.; Frank, N.; Edgerton, E. S.; Weber, R. J. Water-soluble organic aerosol material and the light-absorption characteristics of aqueous extracts measured over the Southeastern United States. *Atmos. Chem. Phys.* **2010**, *10* (13), 5965–5977.
- (11) Chen, Y.; Bond, T. C. Light absorption by organic carbon from wood combustion. *Atmos. Chem. Phys.* **2010**, *10* (4), 1773–1787.
- (12) Lambe, A. T.; Cappa, C. D.; Massoli, P.; Onasch, T. B.; Forestieri, S. D.; Martin, A. T.; Cummings, M. J.; Croasdale, D. R.; Brune, W. H.; Worsnop, D. R.; Davidovits, P. Relationship between oxidation level and optical properties of secondary organic aerosol. *Environ. Sci. Technol.* **2013**, *47* (12), 6349–6357.
- (13) Lee, H. J.; Aiona, P. K.; Laskin, A.; Laskin, J.; Nizkorodov, S. A. Effect of solar radiation on the optical properties and molecular composition of laboratory proxies of atmospheric brown carbon. *Environ. Sci. Technol.* **2014**, *48* (17), 10217–10226.
- (14) Liu, S.; Shilling, J. E.; Song, C.; Hiranuma, N.; Zaveri, R. A.; Russell, L. M. Hydrolysis of organonitrate functional groups in aerosol particles. *Aerosol Sci. Technol.* **2012**, *46* (12), 1359–1369.
- (15) Lin, Y. H.; Budisulistiorini, H.; Chu, K.; Siejack, R. A.; Zhang, H. F.; Riva, M.; Zhang, Z. F.; Gold, A.; Kautzman, K. E.; Surratt, J. D. Light-absorbing oligomer formation in secondary organic aerosol from reactive uptake of isoprene epoxydiols. *Environ. Sci. Technol.* **2014**, *48* (20), 12012–12021.
- (16) Laskin, J.; Laskin, A.; Roach, P. J.; Slysz, G. W.; Anderson, G. A.; Nizkorodov, S. A.; Bones, D. L.; Nguyen, L. Q. High-resolution desorption electrospray ionization mass spectrometry for chemical characterization of organic aerosols. *Anal. Chem.* **2010**, *82* (5), 2048–2058.
- (17) Updyke, K. M.; Nguyen, T. B.; Nizkorodov, S. A. Formation of brown carbon via reactions of ammonia with secondary organic aerosols from biogenic and anthropogenic precursors. *Atmos. Environ.* **2012**, *63*, 22–31.
- (18) Lee, A. K. Y.; Zhao, R.; Li, R.; Liggi, J.; Li, S. M.; Abbatt, J. P. D. Formation of light absorbing organo-nitrogen species from evaporation of droplets containing glyoxal and ammonium sulfate. *Environ. Sci. Technol.* **2013**, *47* (22), 12819–12826.
- (19) Powelson, M. H.; Espelien, B. M.; Hawkins, L. N.; Galloway, M. M.; De Haan, D. O. Brown carbon formation by aqueous-phase carbonyl compound reactions with amines and ammonium sulfate. *Environ. Sci. Technol.* **2014**, *48* (2), 985–993.
- (20) Phillips, S. M.; Smith, G. D. Light absorption by charge transfer complexes in brown carbon aerosols. *Environ. Sci. Technol. Lett.* **2014**, *1* (10), 382–386.
- (21) Sharpless, C. M.; Blough, N. V. The importance of charge-transfer interactions in determining chromophoric dissolved organic matter (CDOM) optical and photochemical properties. *Environ. Sci. Proc. Imp* **2014**, *16* (4), 654–671.
- (22) Laskin, J.; Laskin, A.; Nizkorodov, S. A.; Roach, P.; Eckert, P.; Gilles, M. K.; Wang, B. B.; Lee, H. J.; Hu, Q. C. Molecular selectivity of brown carbon chromophores. *Environ. Sci. Technol.* **2014**, *48* (20), 12047–12055.
- (23) Sareen, N.; Moussa, S. G.; McNeill, V. F. Photochemical aging of light-absorbing secondary organic aerosol material. *J. Phys. Chem. A* **2013**, *117* (14), 2987–2996.
- (24) Zhao, R.; Lee, A. K. Y.; Huang, L.; Li, X.; Yang, F.; Abbatt, J. P. D. Photochemical processing of aqueous atmospheric brown carbon. *Atmos. Chem. Phys.* **2015**, *15* (11), 6087–6100.
- (25) Rincon, A. G.; Guzman, M. I.; Hoffmann, M. R.; Colussi, A. J. Thermochromism of model organic aerosol matter. *J. Phys. Chem. Lett.* **2010**, *1* (1), 368–373.
- (26) De Haan, D. O.; Hawkins, L. N.; Kononenko, J. A.; Turley, J. J.; Corrigan, A. L.; Tolbert, M. A.; Jimenez, J. L. Formation of nitrogen-containing oligomers by methylglyoxal and amines in simulated evaporating cloud droplets. *Environ. Sci. Technol.* **2011**, *45* (3), 984–991.
- (27) Nguyen, T. B.; Lee, P. B.; Updyke, K. M.; Bones, D. L.; Laskin, J.; Laskin, A.; Nizkorodov, S. A. Formation of nitrogen- and sulfur-containing light-absorbing compounds accelerated by evaporation of water from secondary organic aerosols. *J. Geophys. Res.* **2012**, *117*, (D1), D01207, DOI: [10.1029/2011JD016944](https://doi.org/10.1029/2011JD016944).
- (28) Feng, Y.; Ramanathan, V.; Kotamarthi, V. R. Brown carbon: a significant atmospheric absorber of solar radiation? *Atmos. Chem. Phys.* **2013**, *13* (17), 8607–8621.
- (29) Nozière, B.; Kalberer, M.; Claeys, M.; Allan, J.; D'Anna, B.; Decesari, S.; Finessi, E.; Glasius, M.; Grgić, I.; Hamilton, J. F.; Hoffmann, T.; Iinuma, Y.; Jaoui, M.; Kahnt, A.; Kampf, C. J.; Kourtchev, I.; Maenhaut, W.; Marsden, N.; Saarikoski, S.; Schnelle-Kreis, J.; Surratt, J. D.; Szidat, S.; Szmigielski, R.; Wisthaler, A. The molecular identification of organic compounds in the atmosphere: state of the art and challenges. *Chem. Rev.* **2015**, *115* (10), 3919–3983.
- (30) Desyaterik, Y.; Sun, Y.; Shen, X. H.; Lee, T. Y.; Wang, X. F.; Wang, T.; Collett, J. L. Speciation of "brown" carbon in cloud water impacted by agricultural biomass burning in eastern China. *J. Geophys. Res.-Atmos* **2013**, *118* (13), 7389–7399.
- (31) Claeys, M.; Vermeylen, R.; Yasmeen, F.; Gomez-Gonzalez, Y.; Chi, X. G.; Maenhaut, W.; Meszaros, T.; Salma, I. Chemical characterisation of humic-like substances from urban, rural and tropical biomass burning environments using liquid chromatography with UV/vis photodiode array detection and electrospray ionisation mass spectrometry. *Environ. Chem.* **2012**, *9* (3), 273–284.
- (32) Kitanovski, Z.; Grgic, I.; Vermeylen, R.; Claeys, M.; Maenhaut, W. Liquid chromatography tandem mass spectrometry method for characterization of monoaromatic nitro-compounds in atmospheric particulate matter. *J. Chromatogr A* **2012**, *1268*, 35–43.

- (33) Kitanovski, Z.; Grgic, I.; Yasmeen, F.; Claeys, M.; Cusak, A. Development of a liquid chromatographic method based on ultraviolet-visible and electrospray ionization mass spectrometric detection for the identification of nitrocatechols and related tracers in biomass burning atmospheric organic aerosol. *Rapid Commun. Mass Spectrom.* **2012**, *26* (7), 793–804.
- (34) Zhang, X. L.; Lin, Y. H.; Surratt, J. D.; Weber, R. J. Sources, composition and absorption angstrom exponent of light-absorbing organic components in aerosol extracts from the Los Angeles Basin. *Environ. Sci. Technol.* **2013**, *47* (8), 3685–3693.
- (35) Zhang, X. L.; Lin, Y. H.; Surratt, J. D.; Zotter, P.; Prevot, A. S. H.; Weber, R. J. Light-absorbing soluble organic aerosol in Los Angeles and Atlanta: A contrast in secondary organic aerosol. *Geophys. Res. Lett.* **2011**, *38* (21), L21810, DOI: [10.1029/2011GL049385](https://doi.org/10.1029/2011GL049385).
- (36) Lin, P.; Liu, J. M.; Shilling, J. E.; Kathmann, S. M.; Laskin, J.; Laskin, A. Molecular characterization of brown carbon (BrC) chromophores in secondary organic aerosol generated from photo-oxidation of toluene. *Phys. Chem. Chem. Phys.* **2015**, *17*, 23312.
- (37) Nguyen, T. B.; Laskin, A.; Laskin, J.; Nizkorodov, S. A. Brown carbon formation from ketoaldehydes of biogenic monoterpenes. *Faraday Discuss.* **2013**, *165*, 473–494.
- (38) Galloway, M. M.; Powelson, M. H.; Sedehi, N.; Wood, S. E.; Millage, K. D.; Kononenko, J. A.; Rynaski, A. D.; De Haan, D. O. Secondary organic aerosol formation during evaporation of droplets containing atmospheric aldehydes, amines, and ammonium sulfate. *Environ. Sci. Technol.* **2014**, *48* (24), 14417–14425.
- (39) Kroll, J. H.; Ng, N. L.; Murphy, S. M.; Varutbangkul, V.; Flagan, R. C.; Seinfeld, J. H. Chamber studies of secondary organic aerosol growth by reactive uptake of simple carbonyl compounds. *J. Geophys. Res.* **2005**, *110*, (D23), D23207, DOI: [10.1029/2005JD006004](https://doi.org/10.1029/2005JD006004).
- (40) Sareen, N.; Schwier, A. N.; Shapiro, E. L.; Mitroo, D.; McNeill, V. F. Secondary organic material formed by methylglyoxal in aqueous aerosol mimics. *Atmos. Chem. Phys.* **2010**, *10* (3), 997–1016.
- (41) Sedehi, N.; Takano, H.; Blasic, V. A.; Sullivan, K. A.; De Haan, D. O. Temperature- and pH-dependent aqueous-phase kinetics of the reactions of glyoxal and methylglyoxal with atmospheric amines and ammonium sulfate. *Atmos. Environ.* **2013**, *77*, 656–663.
- (42) Drozd, G. T.; McNeill, V. F. Organic matrix effects on the formation of light-absorbing compounds from alpha-dicarbonyls in aqueous salt solution. *Environ. Sci.-Proc. Imp* **2014**, *16* (4), 741–747.
- (43) Kampf, C. J.; Jakob, R.; Hoffmann, T. Identification and characterization of aging products in the glyoxal/ammonium sulfate system - implications for light-absorbing material in atmospheric aerosols. *Atmos. Chem. Phys.* **2012**, *12* (14), 6323–6333.
- (44) Tang, I. N.; Munkelwitz, H. R. Water activities, densities, and refractive-indexes of aqueous sulfates and sodium-nitrate droplets of atmospheric importance. *J. Geophys. Res.* **1994**, *99* (D9), 18801–18808.
- (45) Matsunaga, S.; Mochida, M.; Kawamura, K. Variation on the atmospheric concentrations of biogenic carbonyl compounds and their removal processes in the northern forest at Moshiri, Hokkaido Island in Japan. *J. Geophys. Res.* **2004**, *109*, (D4), D04302, DOI: [10.1029/2003JD004100](https://doi.org/10.1029/2003JD004100).
- (46) Seinfeld, J. H.; Pandis, S. N. *Atmospheric Chemistry and Physics: From Air Pollution to Climate Change*, 2<sup>nd</sup> ed.; Wiley-Interscience: New York, 2006, 1203 pages.
- (47) Jaitly, N.; Mayampurath, A.; Littlefield, K.; Adkins, J. N.; Anderson, G. A.; Smith, R. D. Decon2LS: An open-source software package for automated processing and visualization of high resolution mass spectrometry data. *BMC Bioinf.* **2009**, *10*, 87.
- (48) Roach, P. J.; Laskin, J.; Laskin, A. Higher-order mass defect analysis for mass spectra of complex organic mixtures. *Anal. Chem.* **2011**, *83* (12), 4924–4929.
- (49) Eckert, P. A.; Roach, P. J.; Laskin, A.; Laskin, J. Chemical characterization of crude petroleum using nanospray desorption electrospray ionization coupled with high-resolution mass spectrometry. *Anal. Chem.* **2012**, *84* (3), 1517–1525.
- (50) Chamseddin, C.; Jira, T. Evaluation of the chromatographic performance of conventional, polar-endcapped and calixarene-bonded stationary phases for the separation of water-soluble vitamins. *Chromatographia* **2013**, *76* (9–10), 449–457.
- (51) Cuyckens, F.; Claeys, M. Optimization of a liquid chromatography method based on simultaneous electrospray ionization mass spectrometric and ultraviolet photodiode array detection for analysis of flavonoid glycosides. *Rapid Commun. Mass Spectrom.* **2002**, *16* (24), 2341–2348.
- (52) Hettiyadura, A. P. S.; Stone, E. A.; Kundu, S.; Baker, Z.; Geddes, E.; Richards, K.; Humphry, T. Determination of atmospheric organosulfates using HILIC chromatography with MS detection. *Atmos. Meas. Tech.* **2015**, *8* (6), 2347–2358.
- (53) Shalazari, M. S.; Ryabtsova, O.; Kahnt, A.; Vermeylen, R.; Herent, M. F.; Quetin-Leclercq, J.; Van der Veken, P.; Maenhaut, W.; Claeys, M. Mass spectrometric characterization of organosulfates related to secondary organic aerosol from isoprene. *Rapid Commun. Mass Spectrom.* **2013**, *27* (7), 784–794.
- (54) Bones, D. L.; Henriksen, D. K.; Mang, S. A.; Gonsior, M.; Bateman, A. P.; Nguyen, T. B.; Cooper, W. J.; Nizkorodov, S. A. Appearance of strong absorbers and fluorophores in limonene-O<sub>3</sub> secondary organic aerosol due to NH<sub>4</sub><sup>+</sup>-mediated chemical aging over long time scales. *J. Geophys. Res.* **2010**, *115*, (D5), D05203, DOI: [10.1029/2009JD012864](https://doi.org/10.1029/2009JD012864).
- (55) Galloway, M. M.; Loza, C. L.; Chhabra, P. S.; Chan, A. W. H.; Yee, L. D.; Seinfeld, J. H.; Keutsch, F. N. Analysis of photochemical and dark glyoxal uptake: Implications for SOA formation. *Geophys. Res. Lett.*, **2011**, *38*, L17811, DOI: [10.1029/2011GL048514](https://doi.org/10.1029/2011GL048514).
- (56) Yu, G.; Bayer, A. R.; Galloway, M. M.; Korshavn, K. J.; Fry, C. G.; Keutsch, F. N. Glyoxal in aqueous ammonium sulfate solutions: products, kinetics and hydration effects. *Environ. Sci. Technol.* **2011**, *45* (15), 6336–6342.
- (57) Amarnath, V.; Valentine, W. M.; Amarnath, K.; Eng, M. A.; Graham, D. G. The mechanism of nucleophilic-substitution of alkylpyrroles in the presence of oxygen. *Chem. Res. Toxicol.* **1994**, *7* (1), 56–61.
- (58) Layne, J. Characterization and comparison of the chromatographic performance of conventional, polar-embedded, and polar-endcapped reversed-phase liquid chromatography stationary phases. *J. Chromatogr A* **2002**, *957* (2), 149–164.
- (59) Nguyen, T. B.; Nizkorodov, S. A.; Laskin, A.; Laskin, J. An approach toward quantification of organic compounds in complex environmental samples using high-resolution electrospray ionization mass spectrometry. *Anal. Methods* **2013**, *5* (1), 72–80.
- (60) Buck, R. P.; Singhadeja, S.; Rogers, L. B. Ultraviolet absorption spectra of some inorganic ions in aqueous solutions. *Anal. Chem.* **1954**, *26* (7), 1240–1242.
- (61) Cai, Y. Q.; Cai, Y.; Shi, Y. L.; Liu, J. M.; Mou, S. F.; Lu, Y. Q. A liquid-liquid extraction technique for phthalate esters with water-soluble organic solvents by adding inorganic salts. *Microchim. Acta* **2007**, *157* (1–2), 73–79.
- (62) Mopper, K.; Stubbins, A.; Ritchie, J. D.; Bialk, H. M.; Hatcher, P. G. Advanced instrumental approaches for characterization of marine dissolved organic matter: Extraction techniques, mass spectrometry, and nuclear magnetic resonance spectroscopy. *Chem. Rev.* **2007**, *107* (2), 419–442.
- (63) Surratt, J. D.; Kroll, J. H.; Kleindienst, T. E.; Edney, E. O.; Claeys, M.; Sorooshian, A.; Ng, N. L.; Offenberg, J. H.; Lewandowski, M.; Jaoui, M.; Flagan, R. C.; Seinfeld, J. H. Evidence for organosulfates in secondary organic aerosol. *Environ. Sci. Technol.* **2007**, *41* (2), 517–527.
- (64) Galloway, M. M.; Chhabra, P. S.; Chan, A. W. H.; Surratt, J. D.; Flagan, R. C.; Seinfeld, J. H.; Keutsch, F. N. Glyoxal uptake on ammonium sulphate seed aerosol: reaction products and reversibility of uptake under dark and irradiated conditions. *Atmos. Chem. Phys.* **2009**, *9* (10), 3331–3345.
- (65) Loeffler, K. W.; Koehler, C. A.; Paul, N. M.; De Haan, D. O. Oligomer formation in evaporating aqueous glyoxal and methyl glyoxal solutions. *Environ. Sci. Technol.* **2006**, *40* (20), 6318–6323.

(66) Nozriere, B.; Dziedzic, P.; Cordova, A. Products and kinetics of the liquid-phase reaction of glyoxal catalyzed by ammonium ions ( $\text{NH}_4^+$ ). *J. Phys. Chem. A* **2009**, *113* (1), 231–237.

(67) Nozriere, B.; Dziedzic, P.; Cordova, A. Inorganic ammonium salts and carbonate salts are efficient catalysts for aldol condensation in atmospheric aerosols. *Phys. Chem. Chem. Phys.* **2010**, *12* (15), 3864–3872.

(68) Stoll, D. R.; Li, X. P.; Wang, X. O.; Carr, P. W.; Porter, S. E. G.; Rutan, S. C. Fast, comprehensive two-dimensional liquid chromatography. *J. Chromatogr A* **2007**, *1168* (1–2), 3–43.